

Cite this: *Nanoscale*, 2012, **4**, 4587

www.rsc.org/nanoscale

PAPER

Selective hydrogen purification through graphdiyne under ambient temperature and pressure

Steven W. Cranford^{ab} and Markus J. Buehler^{*ab}

Received 17th April 2012, Accepted 27th May 2012

DOI: 10.1039/c2nr30921a

Graphdiyne, a recently synthesized one-atom-thick carbon allotrope, is atomistically porous – characterized by a regular “nanomesh” – and suggests application as a separation membrane for hydrogen purification. Here we report a full atomistic reactive molecular dynamics investigation to determine the selective diffusion properties of hydrogen (H₂) amongst carbon monoxide (CO) and methane (CH₄), a mixture otherwise known as syngas, a product of the gasification of renewable biomass (such as animal wastes). Under constant temperature simulations, we find the mass flux of hydrogen molecules through a graphdiyne membrane to be on the order of 7 to 10 g cm⁻² s⁻¹ (between 300 K and 500 K), with carbon monoxide and methane remaining isolated. Using a simple Arrhenius relation, we determine the energy required for permeation on the order of 0.11 ± 0.03 eV for single H₂ molecules. We find that addition of marginal applied force (approximately 1 to 2 pN per molecule, representing a controlled pressure gradient, ΔP , on the order of 100 to 500 kPa) can successfully enhance the separation of hydrogen gas. Addition of larger driving forces (50 to 100 pN per molecule) is required to selectively filter carbon monoxide or methane, suggesting that, under near-atmospheric conditions, only hydrogen gas will pass such a membrane. Graphdiyne provides a unique, chemically inert and mechanically stable platform facilitating selective gas separation at nominal pressures using a homogeneous material system, without a need for chemical functionalization or the explicit introduction of molecular pores.

1. Introduction

The necessity for clean energy sources and green materials implores a need to recapture (or separate) any by-product of synthesis in an efficient and precise manner, from the macroscale to nanoscale, molecule by molecule. Recently, the ability to separate gaseous mixes by chemical components *via* physical filtration has undergone significant technological advances, through the development of metal–organic frameworks^{1–3} (MOFs), zeolites,^{4,5} and polymeric^{6,7} or biomimetic^{8,9} membranes with chemical specificity.¹⁰ Can a single-phase, chemically homogeneous structure serve the same purpose? The superlative properties and potential applications of synthetic carbon materials – particularly the 2D form of graphene^{11,12} – illustrate their unique scientific and technological importance and have motivated exploration of other potential carbon structures.^{13,14} Naturally occurring carbon exists in only two allotropes,

diamond and graphite, which consist of extended networks of sp³- and sp²-hybridized carbon atoms, respectively.¹³ Other ways to construct carbon allotropes are theoretically possible by altering the periodic binding motif in networks consisting of sp³-, sp²- and sp-hybridized carbon atoms.^{14,15} Graphdiyne – a variation on of the sp² carbon motif forming graphene – has been the subject of continuing interest among structural, theoretical, and synthetic scientists due to its promising electronic, optical, and mechanical properties,^{15–20} as well as recent practical strategies of synthesis.^{15,21–23} Specifically, graphdiyne is a two-dimensional structure of sp–sp²-hybridized carbon atoms (Fig. 1A), which can be thought of as simply linking the characteristic hexagons of graphene by diacetylenic (single- and triple-bond) linkages. The presence of these acetylenic groups in such structures introduces a rich variety of optical and electronic properties that are quite different from those of graphene or carbon nanotubes.^{17,24} From a structural perspective, however, they naturally introduce uniform, repeating triangular atomistic pores, with a van der Waals (vdW) openings on the order of ~6.3 Å² (Fig. 1B). Combined with mono-atomic thickness, it has been suggested that graphdiyne might be successful for hydrogen purification,¹⁶ or correspondingly filtration of other small molecules.

The size of van der Waals (vdW) pores defined by this “nanomesh” falls between the vdW dimension of hydrogen and

^aCenter for Materials Science and Engineering, Massachusetts Institute of Technology, 77 Massachusetts Ave., Cambridge, MA, USA. E-mail: mbuehler@MIT.EDU; Fax: +1-617-324-4014; Tel: +1-617-452-2750

^bLaboratory for Atomistic and Molecular Mechanics, Department of Civil and Environmental Engineering, Massachusetts Institute of Technology, 77 Massachusetts Ave. Room 1-235A&B, Cambridge, MA, USA. Web: <http://web.mit.edu/lmbuehler/www/>

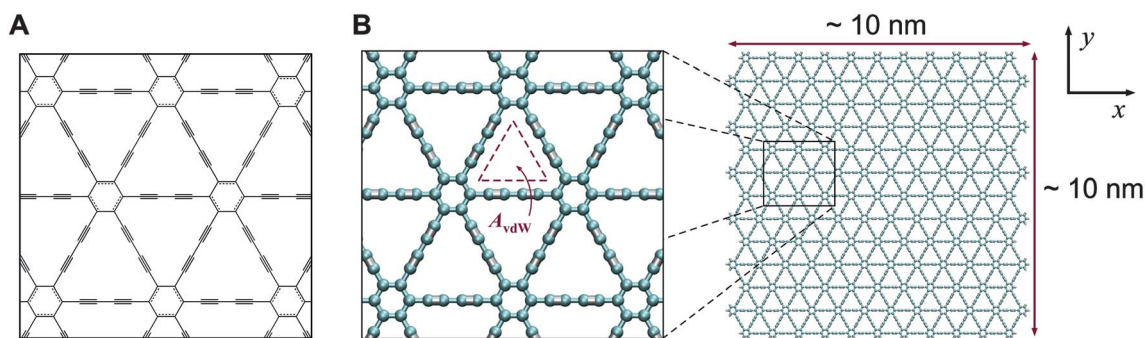


Fig. 1 Schematic and model of graphdiyne. (A) Chemical structure of graphdiyne, a two-dimensional structure of sp-sp²-hybridized carbon atoms with characteristic hexagons of graphene by diacetylenic (single- and triple-bond) linkages forming a repeating and regular nanomesh. (B) Full atomistic model of graphdiyne depicting the atomistic triangular pores, with van der Waals openings (A_{vdW}) on the order of $\sim 6.3 \text{ \AA}^2$. The graphdiyne membrane employed here has dimensions on the order of $10 \text{ nm} \times 10 \text{ nm}$ (approximately 250 exposed pores); graphdiyne edges are terminated with hydrogen atoms for stability.

methane/carbon monoxide, suggesting possible utilization as a separation membrane for hydrogen purification from *syngas* – a mix of H₂, CH₄, and CO, commonly produced by the partial oxidation of methane,²⁵ as well as the gasification of renewable biomass^{26,27} (such as animal waste²⁸ and sewage sludge²⁹). The main components of *syngas* can be converted to valuable products.³⁰ As the permeance of a membrane is inversely proportional to its thickness,³¹ several atomistically thin porous structures aimed for gas separation have been proposed, for example functionalized porous graphene,^{32–35} multilayer carbon-based membranes,^{36–38} or nanoporous silica.^{39–41}

The effective pore size of graphdiyne can be determined by taking by the van der Waals diameter of the acetylene carbon links, resulting in a triangular pore with a length of $\sim 3.8 \text{ \AA}$ (as previously reported;¹⁶ easily calculated by the geometry of graphdiyne). The kinetic diameter of the gases are $\sim 2.93 \text{ \AA}$, $\sim 3.76 \text{ \AA}$, and $\sim 3.83 \text{ \AA}$ for H₂, CO, and CH₄ respectively.⁴² By geometric arguments alone, graphdiyne appears ideally suited for H₂ filtration. Yet the triangular shape of the pore would impede free passage (even for such nonpolar molecules), and one would anticipate an energetic penalty. Moreover, even the weak van der Waals interactions extend beyond the ideal cutoff, and the multibody interactions of the gaseous mix may result in deviations from the ideal kinetic diameters (*e.g.*, local temperature fluctuations). Thus, while the pore size and kinetic diameters are compatible, we define the filtration in terms of chemical selectivity *via* definition of energy barriers, in a general approach. As such, similar concepts can be invoked in future studies (such as filtration of polar water molecules, *etc.*)

2. Materials and methods

While graphdiyne has only been recently synthesized atop copper substrates,^{21,22} recent theoretical and full atomistic studies suggest that freestanding mono-atomistic graphdiyne layers would not only be chemically stable,^{43,44} but also achieve strength on the order of 40 GPa.^{43,45} Being said, until such materials are characterized experimentally, the strength remains a theoretical prediction. Combined with the chemical inertness of pure carbon, such a material would provide a robust platform for repeatable gas separation. We explore the relative selectivity of

H₂, CH₄, and CO using a full atomistic molecular dynamics (MD) approach, which allows for the simulation of large systems and a direct analysis of the molecular dynamics of the process.

2.1 Force field, time step and thermostat

The full atomistic investigations utilize the first-principles-based ReaxFF potential, originally developed for hydrocarbon systems,⁴⁶ providing an MD framework for chemical and mechanical behavior with near quantum-chemical accuracy. The version of the ReaxFF force field used here is that reported by Chenoweth and van Duin *et al.*⁴⁷ The time step is chosen to be on the order of a fraction of femtoseconds ($0.1 \times 10^{-15} \text{ s}$), to ensure the stability of the simulations and reflect the relatively high vibrational frequency of the triple-bonded acetylenic groups and relatively low-mass H₂ molecules. All full atomistic simulations are subject to a microcanonical (NVT) ensemble, carried out at temperatures from 300 K to 500 K (we note while *syngas* is synthesized at temperatures on the order of 1000 K,^{27,28} our intent is to model the downstream filtration of such a gas, to recapture H₂ and separate heavier molecules). This temperature range further ensures mechanical stabilization of the atomistic membrane. Temperature control was achieved using a Berendsen thermostat, with a damping parameter of 1.0 fs (10 time steps) to maintain near constant temperature. All simulations are performed using the massively parallelized modeling code LAMMPS (<http://lammps.sandia.gov/>).⁴⁸

2.2 Geometry, gas mix, and boundary conditions

For the simulation configuration, an approximately square sheet of graphdiyne ($10.6 \text{ nm} \times 11.2 \text{ nm}$) serves as a mono-atomistic membrane. The edges of the graphdiyne sheet were terminated with hydrogen to ensure stability, similar to other all-carbon-based structures.^{43,49} The membrane separates a gaseous mix of H₂, CO, and CH₄, or *syngas*, (consisting of 400 H₂ molecules, 400 CO molecules, and 200 CH₄ molecules, a molar ratio of 2 : 2 : 1, independently equilibrated at 300 K for 50 ps, or 500 000 integration steps) from a vacuum.

The initial gaseous mix (or “reservoir”) has a finite pressure, and thus an implicit pressure gradient between the “reservoir” and the “vacuum” that is temperature dependent. For example,

at 300 K the reservoir pressure is approximately 5 atm. Using an NVT ensemble for the simulations, volume and temperature were kept constant, and as a result, the pressure at the “reservoir” side (where the bulk of the gas remains) is free to change throughout the simulation(s). This change, however, is minimal, as the pressure is dominated by the much heavier CO and CH₄ molecules, and the removal of a few H₂ molecules is effectively negligible. Indeed, even at 500 K, less than 10% of the total H₂ molecules pass the membrane (less than 1% of the gas admixture by weight). Attempting to maintain constant reservoir pressure with a finite number of atoms effectively prescribes a necessary reservoir size (such that the removal of H₂ does not cause great changes in pressure) as well as a limiting simulation time (such that the amount of removed H₂ does not greatly change the relative concentration). Compared to experimental values, the ratio of methane used here is larger than typical, depending on the syngas source.^{27,28} Due to the prevalence of the simple reaction pathway $C + H_2O \rightarrow CO + H_2$ in the pyrolysis of biodiesel for example,²⁷ a 1 : 1 molar ratio of H₂ and CO, with the combination thereof constituting the majority of the gaseous mix, is deemed sufficient to delineate chemical permittivity. Boundaries are periodic at the limits of the graphdiyne plane, and fixed normal to the plane (depicted in Fig. 2). The upper/lower boundaries induce a harmonic force, such that the molecules reflect back towards the system upon contact.

3. Results and discussion

3.1 Temperature dependence

Upon simulation at finite temperature (300 K), hydrogen molecules are able to intermittently traverse the graphdiyne membrane, while the larger CO and CH₄ molecules are impeded. Not all H₂ molecules successfully pass through the pores, suggesting a nominal energy barrier. A recent investigation reported a density functional theory (DFT) and transition state theory (TST) study on gas diffusion through graphdiyne,¹⁶ and provided the first predictions of the hydrogen diffusion rate and selectivity to CH₄/CO. However, due to the limitations of DFT, only the energy required for single molecules directly traversing a graphdiyne pore was delineated. Indeed, the energy barriers for H₂, CO and CH₄ passing through the graphdiyne pores were computed to be 0.10, 0.33 and 0.72 eV, respectively.¹⁶ This barrier for H₂ diffusion is relatively surmountable compared to CH₄/CO, and is much smaller than that across the previously published porous graphene (on the order of 0.2 eV to 0.6 eV (ref. 32–35)). Currently, the mechanical behavior of a much larger system of graphdiyne–syngas, as well as the potential limiting effects of a mixed gaseous system (*e.g.*, involving H₂–CO–CH₄ interactions) remains unknown and requires system scales larger than accessible by DFT, suggesting the full atomistic molecular modeling approach hence undertaken. Rather than characterizing the energy barriers of individual molecules in isolation and extrapolating the selectivity and gas diffusion rate *via* transition state theory,^{16,38} full atomistic molecular modeling allow the explicit measurement of diffusion rates across a range of finite temperatures in larger systems (albeit still limited to nanoscale dimensions). As such, an atomistic model more accurately

represents the stochastic nature of the physical system, providing a statistical range of values.

Commonly, Knudsen diffusion⁵⁰ or molecular (Fickian) diffusion⁵¹ is used to quantify gas separation as most membranes with finite thickness consist of relatively long pores (compared to molecular diameter), and the mean free path of a traversing molecule is a more relevant metric to describe permittivity.⁵² Here, the filtration process consists of a single molecule traversing a mono-atomistic membrane, theoretically described by single, finite and constant energy barrier at the pore (dependent on the target molecule). As such, diffusion can be successfully described by an Arrhenius relation, where $A = A_0 \exp[-E_0/k_B T]$, for which A is the diffusion rate, A_0 is the diffusion pre-factor, E_0 the energy required to permeate (depicted schematically in Fig. 3A), k_B the Boltzmann constant, and T the temperature. In general, the Arrhenius relation accounts for the temperature dependence on reaction rates. Here, we amend the general relation to account for the discrete kinetic energy of each molecule (where $2K = mv^2$) and the relation between temperature and kinetic energy is simply:

$$k_B T = 2\bar{K}/(3N). \quad (1)$$

Here, \bar{K} indicates the average kinetic energy of a sample of molecules, N . Due to the assignment of atomistic velocities and fixed thermostatting, the above relation holds for any arbitrary subset of molecules. Rearranging as a function of temperature:

$$\frac{1}{k_B T} = -\frac{3N}{2E_0} \ln\left(\frac{A}{A_0}\right) = -\frac{3N}{2E_0} \ln(\eta) + C(A_0, E_0), \quad (2)$$

where C is a fitted constant, a function of A_0 and E_0 . Here, we explicitly calculate η in terms of the mass flux ($\text{g cm}^{-2} \text{s}^{-1}$) by determining the total number of H₂ molecules passing through the graphdiyne membrane for variations in temperature (example shown in Fig. 3B for $T = 500$ K). We further note that the mass flux, η , is not a direct measure of successful passages (*e.g.*, the energy barrier defined by permeating a single molecule through a single pore). Rather, η captures the quantity of H₂ that completely escapes interaction with the graphdiyne plane and thus successfully isolated from the syngas–membrane system. For example, a H₂ molecule may pass through the plane, reverse trajectories (due to thermal fluctuations) and permeate back to the syngas “reservoir” – while successfully overcoming the energy barrier, the molecule has not been isolated.

To measure the flux, the system is subject to finite temperature for a time period of 50 ps, and the number of hydrogen molecules, n , successfully escaping calculated. Again, aside from computational efficiency, a relatively short time period is used as, upon separation through the membrane, there is less concentration of H₂ (due to the fixed number of atoms/molecules within the system) among the syngas. Simulations are repeated four times for each temperature (300 K, 350 K, 400 K, 450 K, and 500 K) to attain statistical variation, and an average flux, $\bar{\eta}$, determined. The determined mass transfer ranged from $\bar{\eta} \approx 7.3 \text{ g cm}^{-2} \text{ s}^{-1}$ at 300 K to $\bar{\eta} \approx 9.4 \text{ g cm}^{-2} \text{ s}^{-1}$ at 500 K – an increase of approximately 30%. Temperature dependence is determined by plotting $1/k_B T$ versus $\ln(\eta)$ (see Fig. 3C). From the relation given (eqn (2)), the energy barrier per hydrogen molecule is calculated to be approximately $0.11 \pm 0.03 \text{ eV}$, in close agreement with

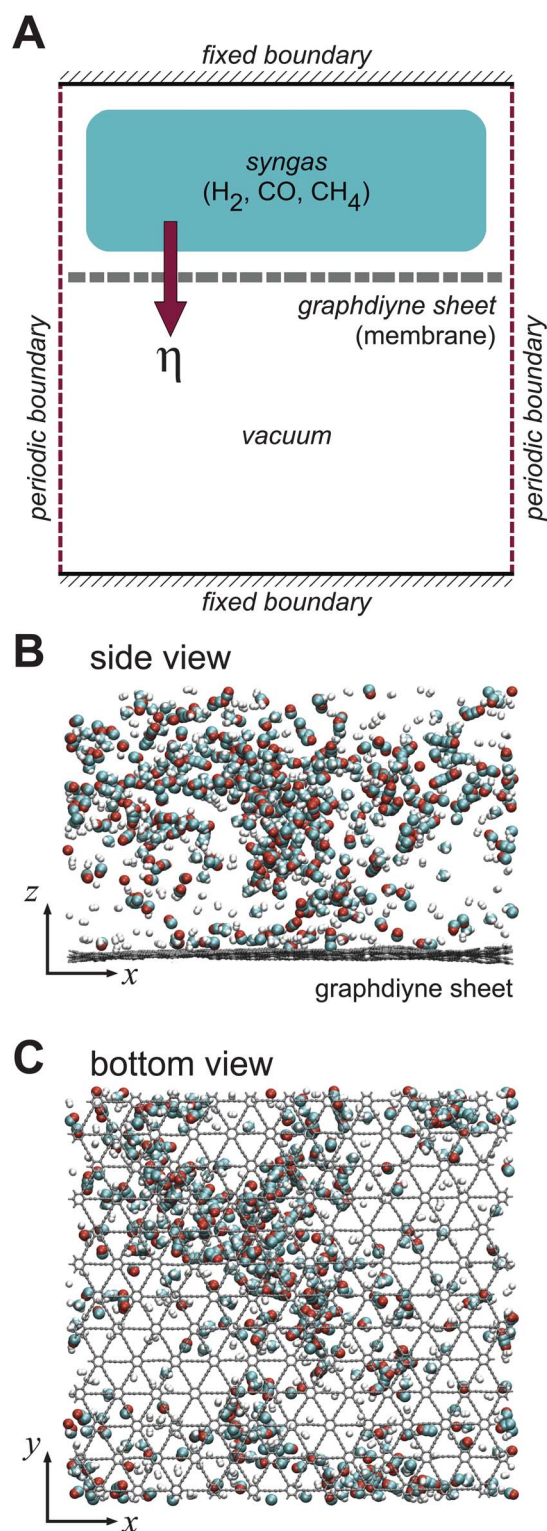


Fig. 2 Schematic and model of membrane–gas system. (A) For the simulation, a sheet of graphdiyne (10.6 nm × 11.2 nm) serves as a monoatomistic membrane, separating a gaseous mix of H₂, CO, and CH₄ from a vacuum (consisting of 400 H₂ molecules, 400 CO molecules, and 200 CH₄ molecules). Boundaries are periodic at the limits of the graphdiyne plane, and fixed normal to the plane. The upper/lower boundaries induce a harmonic force, such that the molecules reflect back towards the system upon contact (closed system). During simulation, the number of hydrogen atoms that permeate across the membrane are used to calculate

previous DFT results (0.10 eV). The small deviation can be attributed to the thermal fluctuations of both the passing H₂ molecule and graphdiyne sheet. It is noted however that this “ground state energy barrier”, E_0 , is the energy barrier for this system (syngas at 5 atm separated from a vacuum, with a H₂ : CO : CH₄ ratio of 2 : 2 : 1). Depending on the stoichiometry and imposed boundary conditions, what constitutes the “ground state conditions” may vary. We further discern, from the temperature–kinetic energy relation (eqn (1)), within a range of 300 K to 500 K, the kinetic energy of molecules of CO and CH₄ is on the order of 0.08–0.13 eV and 0.20–0.32 eV, respectively – inadequate to surmount the energy barriers previously reported (0.33 and 0.72 eV (ref. 16)), even assuming marginal stochastic variation in molecular velocities. In terms of kinetic energy, it would require temperatures on the order of 1100 K to 1300 K to provide CO and CH₄ sufficient energy to traverse the membrane (on the order of the temperatures required for syngas synthesis^{27,28}), significantly increasing the energetic input for efficient filtration. Hydrogen, in contrast, can successfully diffuse at near-atmospheric (or room) temperatures (~300 K).

3.2 Force dependence

Aside from variation in temperature, we further consider that the system can be potentially driven towards the membrane, which serves to decrease the energy barrier for passage (similar to Bell’s model^{53,54} applied to the unfolding of proteins,^{55,56} for example) by:

$$A(f) = A_0 \exp \left[- \frac{E_0 - f \cdot x}{k_B T} \right]. \quad (3)$$

By smartly selecting the driving force, f , the energy barrier for H₂ and CO or CH₄ can be surmounted by design (depicted in Fig. 4A and B), allowing the selective isolation of H₂, CO, and/or CH₄. Rearranging as a function of force yields:

$$f = \frac{k_B T}{x} \ln(\eta) + C(A_0, E_0, x, T). \quad (4)$$

where again, C is a constant dependent on A_0 , E_0 , x , and T . For this case, a constant temperature of 300 K is used, such that $k_B T$ (or, similarly, the kinetic energy, \bar{K}) is a constant. Again, we note that the force effectively adds a bias to the system ground state, and is dependent on initial conditions (volume, temperature, stoichiometry, *etc.*). As an initial estimate of necessary force magnitude, from the aforementioned DFT study, the distance required to escape interaction with the graphdiyne sheet is on the order of 4 Å for H₂. Letting $f \cdot x = E_0$, and $x \approx 4$ Å results in a force on the order of 0.025 eV/Å (approximately 40 pN) to facilitate permeation of hydrogen (in the absence of temperature). As H₂ intermittently exceeds the energy barrier in the absence of force (e.g., $\eta \approx 7$ g cm⁻² s⁻¹ at a finite temperature of 300 K), the necessary force is less than the calculated value of approximately 40 pN (indeed, all H₂ would pass at such a high applied force). During simulation, forces were added to the

the mass flux, η . (B) Side view of full atomistic model (initial conditions at $t = 0$). (C) Bottom view (from below graphdiyne membrane) of full atomistic model (initial conditions at $t = 0$).

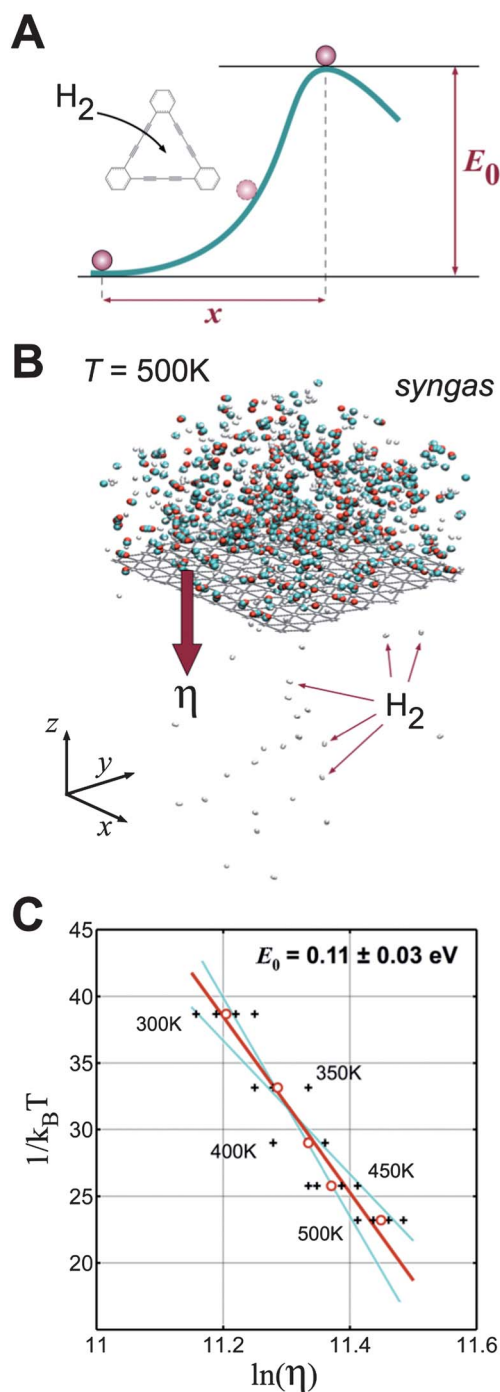


Fig. 3 Temperature variation and energy barrier calculation. (A) Schematic of the energy barrier required for H_2 to successfully pass through graphdiyne; basis of the Arrhenius relation. (B) Simulation snapshot for $T = 500 \text{ K}$, $t = 30 \text{ ps}$, $n \approx 30 \text{ H}_2$ molecules. (C) Temperature dependence on flux, η . Simulations are repeated at temperatures of 300 K, 350 K, 400 K, 450 K, and 500 K (crosses) to attain statistical variation, and an average flux, $\bar{\eta}(T)$ determined (circles). From the relation given in eqn (2), the energy barrier per hydrogen molecule is calculated to be approximately $0.11 \pm 0.03 \text{ eV}$ (variance of fit depicted by dashed lines).

molecules on the order of 0.5 to 3.0 pN to represent a controlled pressure gradient within a range of approximately 100 to 500 kPa (by a virial assumption that $\Delta P = V^{-1} \sum \hat{r}_z \cdot f$, where \hat{r}_z is the

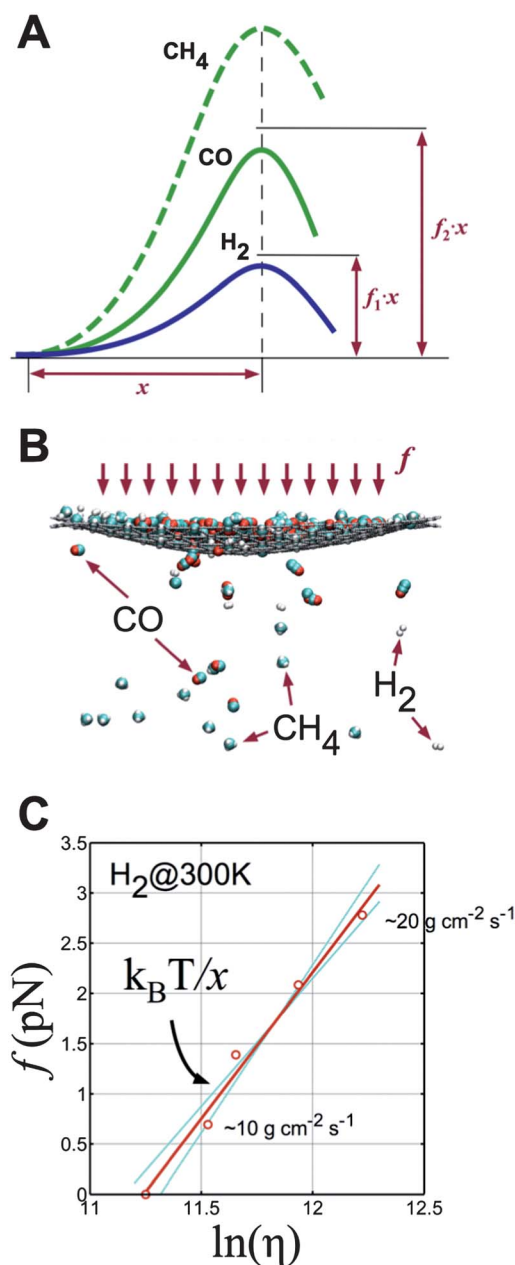


Fig. 4 Variation of applied force at constant temperature (300 K). (A) Application of additional force can reduce the energy requirement to traverse the graphdiyne membrane, allowing the potential for selective filtration at critical force levels. (B) Simulation snapshot for $T = 300 \text{ K}$ and a molecular force of $f \approx 70 \text{ pN}$. Both CO and CH_4 successfully pass the membrane along with H_2 . All hydrogen is driven through the membrane. (C) Investigation of smaller force regime (up to approximately 3 pN) to quantify enhancement of hydrogen diffusion under nominal forces (no passage of CO/ CH_4). Mass flux increased from approximately $7 \text{ g cm}^{-2} \text{ s}^{-1}$ ($f = 0$) to $20 \text{ g cm}^{-2} \text{ s}^{-1}$ ($f = 2.8$), representing a marginal pressure difference, ΔP , of 500 kPa ($\sim 5 \text{ bar}$). The escape distance for hydrogen, x , is calculated to be $9.5 \pm 1.4 \text{ \AA}$.

unit vector in the direction of the applied force), to enhance successful permeation (Fig. 4C).

As anticipated, nominal additional force resulted in a higher yield of H_2 , increasing the flux, η , from $\sim 10 \text{ g cm}^{-2} \text{ s}^{-1}$ at $f \approx 0.7 \text{ pN}$ to $\sim 20 \text{ g cm}^{-2} \text{ s}^{-1}$ at $f \approx 2.8 \text{ pN}$. Moreover, the escape

distance for hydrogen, x , was calculated to be $9.5 \pm 1.4 \text{ \AA}$, larger than previously reported – however, due to the larger fluctuating graphdiyne system, the presence numerous gas molecules, and the definition of isolation, it is expected the membrane influence (represented by x) would increase. At an applied force of $\sim 14 \text{ pN}$, almost all of the hydrogen was successfully removed from the initial syngas mix while CO/CH₄ were still impeded. While delineation of rates becomes difficult to quantify (due to all H₂ molecules passing in the limited molecular sample), applied force was incrementally increased until both CO and CH₄ successfully traversed the membrane. At a critical force range of approximately 55 to 70 pN, CO molecules began to pass the graphdiyne sheet, while a higher range of 70 to 85 pN was required to initial permeation of CH₄. Assuming an escape distance, x , of similar magnitude to hydrogen ($\sim 10 \text{ \AA}$), and the kinetic energy at 300 K, the energy barriers can be estimated (where $E_0 \cong K + f \cdot x$), resulting in 0.42 to 0.52 eV for CO and 0.54 to 0.72 eV for CH₄, again, in close agreement with previously reported DFT results (0.33 eV and 0.72 eV for CO and CH₄ respectively¹⁶). Using the same virial pressure calculation, these critical forces are equal to pressure differences on the order of 200 MPa – much higher than required for hydrogen gas. Once more, hydrogen is successfully diffused at near-atmospheric pressures ($\sim 100 \text{ kPa}$). It is noted, however, that for all cases, the graphdiyne sheet maintained structural integrity, suggesting that even high pressure separation could be mechanically feasible (while requiring significantly more work to achieve).

Regardless of the current imposed conditions (*e.g.*, molar concentration of gases), the additional force can be considered an energetic bias in addition to the finite temperature existing pressure difference (between the “reservoir” and the “vacuum”), both of which can serve to enhance hydrogen permittivity. While such a bias effectively (and predictably) decreases the energy barrier, a one-to-one mapping this effect into physical conditions is more challenging (*e.g.*, a pressure gradient would not impose constant forces on each individual molecule). The key result is that very little “push” is required (from an energetic perspective) to enhance hydrogen filtration while segregating heavier molecules, on the order of hundreds of kPa. In effect, the addition of force (or pressure) quantifies the margin of variation which one can filter hydrogen (another route, of course, being direct control of temperature, also coupled with the gas pressure). Being said, an effective applied (and additional) pressure difference of $\sim 1 \text{ atm}$ seems more energetically efficient than a temperature increase of $\sim 200 \text{ K}$ (with comparable results).

4. Conclusion

Here, full atomistic molecular dynamics was employed to observe the mechanism of diffusion of hydrogen molecules at physical time scales and at finite temperatures and pressures, allowing for the direct calculation of mass flux under stochastic conditions. We have shown that, due to an intrinsic nanomesh structure, atomistically large sheets of graphdiyne can be potentially employed as a successful membrane for hydrogen gas separation from a combined system of hydrogen, carbon monoxide and methane – a gaseous admixture otherwise known as syngas. Complementary to previous DFT investigations,¹⁶ we have shown that the necessary energy for H₂ to traverse

a graphdiyne sheet can be attained at standard temperature and pressure (STP) conditions ($\sim 300 \text{ K}$ and $\sim 100 \text{ kPa}$), suggesting minimal energetic cost for such a membrane. By using finite temperature MD simulations across a temperature range of 300 K to 500 K, we further indicate that graphdiyne acts as a barrier to CO and CH₄ molecules. Permeation of hydrogen can be successfully described by the temperature-dependent Arrhenius relation and extended to account for the application of force, in a manner analogous to Bell’s model, facilitating hydrogen separation, and allowing the filtration of both carbon monoxide and methane at defined pressure levels. In addition, for gas separation applications, one of the critical issues is the mechanical stability of membrane subject to repeatedly imposed pressure differences. Such a concern is negated due to mechanical stability of graphdiyne. Variation of pressure can trigger *selective* permeation of syngas, acting as filter for H₂, or allowing the passage of CO and CH₄. Being said, the promise of mono-atomistic membranes still remains a challenge – even if graphdiyne is highly selective of hydrogen, one cannot expect a successful filtration system with 100 nm² membranes. As H₂ purification is a vital step for the realization of a clean energy economy, combined with recent success synthesis of graphdiyne, such computational results lay the groundwork for compelling new set of experiments that may test the limits of hydrogen selectivity and novel up-scaling of such molecular filtration techniques.

Acknowledgements

This work was supported by the MRSEC Program of the National Science Foundation under award number DMR-0819762. The calculations and the analysis were carried out using a parallelized LINUX cluster at MIT’s Laboratory for Atomistic and Molecular Mechanics (LAMM). Visualization has been carried out using the VMD visualization package.⁵⁷

References

- 1 M. Shah, M. C. McCarthy, S. Sachdeva, A. K. Lee and H. K. Jeong, *Ind. Eng. Chem. Res.*, 2012, **51**, 2179–2199.
- 2 S. T. Meek, J. A. Greathouse and M. D. Allendorf, *Adv. Mater.*, 2011, **23**, 249–267.
- 3 J. R. Li, R. J. Kuppler and H. C. Zhou, *Chem. Soc. Rev.*, 2009, **38**, 1477–1504.
- 4 T. C. Bowen, R. D. Noble and J. L. Falconer, *J. Membr. Sci.*, 2004, **245**, 1–33.
- 5 J. Caro and M. Noack, *Microporous Mesoporous Mater.*, 2008, **115**, 215–233.
- 6 M. Ulbricht, *Polymer*, 2006, **47**, 2217–2262.
- 7 H. Lin and B. D. Freeman, *J. Membr. Sci.*, 2004, **239**, 105–117.
- 8 W. R. Yang, P. J. Lopez and G. Rosengarten, *Analyst*, 2011, **136**, 42–53.
- 9 A. Mecke, C. Dittrich and W. Meier, *Soft Matter*, 2006, **2**, 751–759.
- 10 D. L. Gin and R. D. Noble, *Science*, 2011, **332**, 674–676.
- 11 K. S. Novoselov, A. K. Geim, S. V. Morozov, D. Jiang, Y. Zhang, S. V. Dubonos, I. V. Grigorieva and A. A. Firsov, *Science*, 2004, **306**, 666–669.
- 12 A. K. Geim and K. S. Novoselov, *Nat. Mater.*, 2007, **6**, 183–191.
- 13 A. Hirsch, *Nat. Mater.*, 2010, **9**, 868–871.
- 14 F. Diederich and M. Kivala, *Adv. Mater.*, 2010, **22**, 803–812.
- 15 M. M. Haley, *Pure Appl. Chem.*, 2008, **80**, 519–532.
- 16 Y. Jiao, A. J. Du, M. Hankel, Z. H. Zhu, V. Rudolph and S. C. Smith, *Chem. Commun.*, 2011, **47**, 11843–11845.
- 17 L. D. Pan, L. Z. Zhang, B. Q. Song, S. X. Du and H. J. Gao, *Appl. Phys. Lett.*, 2011, **98**, 173102.

- 18 M. Q. Long, L. Tang, D. Wang, Y. L. Li and Z. G. Shuai, *ACS Nano*, 2011, **5**, 2593–2600.
- 19 G. X. Li, Y. L. Li, X. M. Qian, H. B. Liu, H. W. Lin, N. Chen and Y. J. Li, *J. Phys. Chem. C*, 2011, **115**, 2611–2615.
- 20 G. F. Luo, X. M. Qian, H. B. Liu, R. Qin, J. Zhou, L. Z. Li, Z. X. Gao, E. G. Wang, W. N. Mei, J. Lu, Y. L. Li and S. Nagase, *Phys. Rev. B: Condens. Matter Mater. Phys.*, 2011, **84**, 075439.
- 21 G. X. Li, Y. L. Li, H. B. Liu, Y. B. Guo, Y. J. Li and D. B. Zhu, *Chem. Commun.*, 2010, **46**, 3256–3258.
- 22 X. Qian, Z. Ning, Y. Li, H. Liu, C. Ouyang, Q. Chen and Y. Li, *Dalton Trans.*, 2012, **41**, 730–733.
- 23 S. Wang, L. X. Yi, J. E. Halpert, X. Y. Lai, Y. Y. Liu, H. B. Cao, R. B. Yu, D. Wang and Y. L. Li, *Small*, 2012, **8**, 265–271.
- 24 J. Kang, J. B. Li, F. M. Wu, S. S. Li and J. B. Xia, *J. Phys. Chem. C*, 2011, **115**, 20466–20470.
- 25 J. H. Lunsford, *Catal. Today*, 2000, **63**, 165–174.
- 26 A. M. Henstra, J. Sipma, A. Rinzema and A. J. M. Stams, *Curr. Opin. Biotechnol.*, 2007, **18**, 200–206.
- 27 T. Valliyappan, N. N. Bakhshi and A. K. Dalai, *Bioresour. Technol.*, 2008, **99**, 4476–4483.
- 28 P. De Filippis, C. Borgianni, M. Paolucci and F. Pochetti, *Waste Manage.*, 2004, **24**, 633–639.
- 29 A. Dominguez, Y. Fernandez, B. Fidalgo, J. J. Pis and J. A. Menendez, *Chemosphere*, 2008, **70**, 397–403.
- 30 J. J. Spivey and A. Egbebi, *Chem. Soc. Rev.*, 2007, **36**, 1514–1528.
- 31 S. T. Oyama, D. Lee, P. Hacarlioglu and R. F. Saraf, *J. Membr. Sci.*, 2004, **244**, 45–53.
- 32 Y. F. Li, Z. Zhou, P. W. Shen and Z. F. Chen, *Chem. Commun.*, 2010, **46**, 3672–3674.
- 33 S. Blankenburg, M. Bieri, R. Fasel, K. Mullen, C. A. Pignedoli and D. Passerone, *Small*, 2010, **6**, 2266–2271.
- 34 A. J. Du, Z. H. Zhu and S. C. Smith, *J. Am. Chem. Soc.*, 2010, **132**, 2876.
- 35 D. E. Jiang, V. R. Cooper and S. Dai, *Nano Lett.*, 2009, **9**, 4019–4024.
- 36 R. R. Nair, H. A. Wu, P. N. Jayaram, I. V. Grigorieva and A. K. Geim, *Science*, 2012, **335**, 442–444.
- 37 S. Karan, S. Samitsu, X. Peng, K. Kurashima and I. Ichinose, *Science*, 2012, **335**, 444–447.
- 38 M. Hankel, H. Zhang, T. X. Nguyen, S. K. Bhatia, S. K. Gray and S. C. Smith, *Phys. Chem. Chem. Phys.*, 2011, **13**, 7834–7844.
- 39 H. B. Park and Y. M. Lee, *Adv. Mater.*, 2005, **17**, 477.
- 40 S. T. Oyama, D. Lee, S. Sugiyama, K. Fukui and Y. Iwasawa, *J. Mater. Sci.*, 2001, **36**, 5213–5217.
- 41 R. M. de Vos and H. Verweij, *Science*, 1998, **279**, 1710–1711.
- 42 J. O. Hirschfelder, C. F. Curtiss, R. B. Bird and University of Wisconsin. Theoretical Chemistry Laboratory, *Molecular Theory of Gases and Liquids*, Wiley, New York, 1965.
- 43 S. W. Cranford and M. J. Buehler, *Carbon*, 2011, **49**, 4111–4121.
- 44 A. N. Enyashin and A. L. Ivanovskii, *Phys. Status Solidi B*, 2011, **248**, 1879–1883.
- 45 Y. Yang and X. Xu, *Comput. Mater. Sci.*, 2012, **61**, 83–88.
- 46 A. C. T. van Duin, S. Dasgupta, F. Lorant and W. A. Goddard, *J. Phys. Chem. A*, 2001, **105**, 9396–9409.
- 47 K. Chenoweth, A. C. T. van Duin and W. A. Goddard, *J. Phys. Chem. A*, 2008, **112**, 1040–1053.
- 48 S. Plimpton, *J. Comput. Phys.*, 1995, **117**, 1–19.
- 49 Z. P. Xu and M. J. Buehler, *ACS Nano*, 2010, **4**, 3869–3876.
- 50 K. Malek and M. O. Coppens, *J. Chem. Phys.*, 2003, **119**, 2801–2811.
- 51 B. Hosticka, P. M. Norris, J. S. Brenizer and C. E. Daitch, *J. Non-Cryst. Solids*, 1998, **225**, 293–297.
- 52 S. Roy, R. Raju, H. F. Chuang, B. A. Cruden and M. Meyyappan, *J. Appl. Phys.*, 2003, **93**, 4870–4879.
- 53 G. I. Bell, *Adv. Appl. Probab.*, 1980, **12**, 566–567.
- 54 E. Evans and K. Ritchie, *Biophys. J.*, 1997, **72**, 1541–1555.
- 55 T. Ackbarow, X. Chen, S. Keten and M. J. Buehler, *Proc. Natl. Acad. Sci. U. S. A.*, 2007, **104**, 16410–16415.
- 56 E. B. Walton, S. Lee and K. J. Van Vliet, *Biophys. J.*, 2008, **94**, 2621–2630.
- 57 W. Humphrey, A. Dalke and K. Schulten, *J. Mol. Graphics*, 1996, **14**, 33.